Asian Journal of Basic Science & Research
Volume 8, Issue 2, Pages 166-180, April-June 2026

Development and Characterization of Insulin-Loaded Collagen Hydrogels as Multifunctional Biomaterials for Advanced Biomedical Applications

Imelda G. Contreras-Agüero[1], Lesly Katleya Usme-Duque[1], Denis A. Cabrera-Munguia[1], Lucía F. Cano-Salazar[1], Tirso E. Flores-Guía[1], Francisco J. Enríquez-Medrano[2], Rebeca Betancourt-Galindo[2], Bertha Puente-Urbina[2] & Jesús A. Claudio-Rizo[1*]

[1]Facultad de Ciencias Químicas, Universidad Autónoma de Coahuila, Ing. J. Cárdenas Valdez S/N, República, 25280, Saltillo, Coahuila, Mexico. [2]Centro de Investigación en Química Aplicada, Blvd. Enrique Reyna Hermosillo 140, Col. San José de los Cerritos, 25294, Saltillo, Coahuila, Mexico. Corresponding Author Email: jclaudio@uadec.edu.mx[*]

DOI: https://doi.org/10.38177/ajbsr.2026.8215

Article Received: 25 April 2026 *Article Accepted: 27 June 2026* *Article Published: 29 June 2026*

ABSTRACT

The behavior of insulin encapsulation within collagen-based hydrogels was investigated to explore their potential for biomedical applications. Incorporating insulin into the hydrogel matrix significantly influenced both structural and functional properties. Increasing the insulin content up to 60 µg per gel accelerated the gelation process and enhanced the swelling capacity, reaching values of up to 3800%. However, optimal crosslinking was observed at lower insulin content (15 µg), suggesting the formation of stabilizing urea-type interactions during simultaneous crosslinking with a bioactive polyurethane component. Morphological analysis revealed that insulin incorporation led to smoother and less porous surfaces, indicating a more compact network structure. Mechanically, insulin-loaded hydrogels exhibited improved resistance, sustaining deformation up to 18% under 3.2 million fatigue cycles, highlighting their durability under repetitive stress conditions. Higher insulin concentrations (30–60 µg) promoted a superabsorbent behavior, with swelling values ranging from 3500% to 5600%, strongly dependent on pH conditions and notably enhanced at skin-relevant pH. In addition, the presence of insulin improved resistance to both hydrolytic degradation and enzymatic biodegradation in the presence of pepsin, with the highest stability observed at 60 µg. The materials demonstrated good hemocompatibility and showed controlled surface erosion upon exposure to simulated body fluids. Interestingly, hydroxyapatite deposition was detected through Alizarin Red staining, with a qualitative increase at higher insulin contents, suggesting potential bioactivity toward mineralization processes. Overall, these findings highlight the multifunctional role of insulin beyond its therapeutic activity, acting as a structural and bioactive modulator in collagen-based hydrogels, opening new opportunities for advanced biomedical applications.

Keywords: Collagen Hydrogels; Insulin Encapsulation; Bioactive Polyurethane; Crosslinking Interactions; Swelling Behavior; Mechanical Stability; Controlled Degradation; Hemocompatibility; Biomineralization; Hydrogel Characterization; Biomedical Applications.

1.0. Introduction

Insulin is one of the most widely used and essential therapeutic proteins in modern biomedicine, playing a central role in the management of diabetes and metabolic disorders [1,2]. Beyond its classical function in glucose regulation, insulin has also shown promising effects in tissue regeneration, wound healing, and cellular signaling [2-4]. However, despite its broad therapeutic relevance, insulin faces important limitations that restrict its full clinical potential [4,5]. Its instability under physiological conditions, susceptibility to enzymatic degradation, and short biological half-life often require frequent administration, which can reduce patient compliance and therapeutic efficiency [6,7].

To overcome these challenges, significant efforts have been directed toward developing advanced delivery systems capable of protecting insulin while enabling controlled and sustained release [7,8]. Among these strategies, encapsulation within hydrogel-based matrices has emerged as a particularly attractive approach [9-11]. Hydrogels provide a hydrated, three-dimensional network that can mimic biological environments, offering protection against degradation while facilitating diffusion-controlled transport [9-11]. When designed appropriately, these systems can also respond to environmental stimuli such as pH, further improving the precision of insulin delivery [9-11].

In this context, bioactive hydrogels based on collagen and polyurethane represent a versatile and highly tunable platform [12,13]. Collagen, as a major component of the extracellular matrix, provides inherent biocompatibility,

biodegradability, and favorable interactions with cells [12,13]. Polyurethane, on the other hand, introduces mechanical robustness and enables precise control over network architecture through chemical crosslinking [11-13]. The combination of both components allows the design of hybrid systems with tailored swelling behavior, degradation rates, and mechanical performance, which are critical parameters for biomedical applications [13]. In addition to serving as delivery vehicles, these hybrid hydrogels offer the possibility of modulating their own structural and functional properties through the incorporation of bioactive molecules [12,13]. In this sense, insulin may play a dual role, not only as a therapeutic agent but also as a modulator of the hydrogel network, influencing crosslinking, morphology, and overall performance.

Therefore, the aim of this work is to investigate the effect of insulin encapsulation on the physicochemical, mechanical, and biological properties of collagen–polyurethane hydrogels. We hypothesize that insulin incorporation can simultaneously enhance the structural integrity, swelling capacity, and degradation resistance of the system, while maintaining its biocompatibility. To test this hypothesis, hydrogels with varying insulin content (15-60 μg/hydrogel) were developed and systematically characterized in terms of gelation behavior, morphology, mechanical response under fatigue, swelling performance under different pH conditions, and stability against hydrolytic and enzymatic degradation. Additionally, their hemocompatibility and potential bioactivity—evidenced by their ability to induce hydroxyapatite deposition—were evaluated to assess their suitability for advanced biomedical applications (Fig. 1).

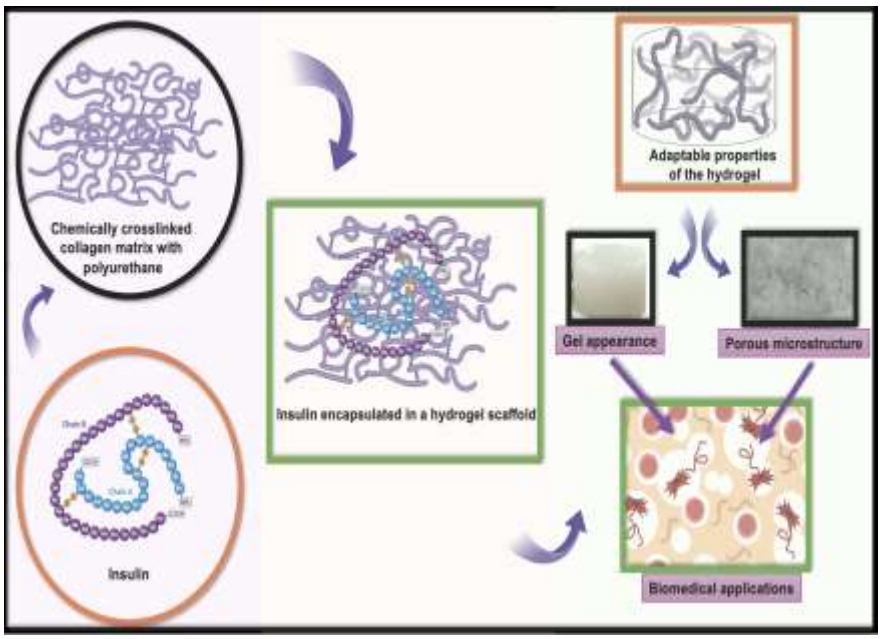

Figure 1. Study design and hypothesis. Insulin-loaded collagen–polyurethane hydrogels are developed to evaluate how insulin content influences the structure, properties, and biomedical potential of the material.

1.1. Study Objectives

The main objectives of this study were:

1) To investigate the physicochemical, structural, and mechanical properties of insulin-loaded collagen–polyurethane hydrogels.

2) To evaluate the effect of insulin incorporation on gelation behavior, network organization, and crosslinking density within the hydrogel matrices.
3) To determine the influence of insulin content on swelling behavior and pH responsiveness under physiologically relevant conditions.
4) To assess the stability of the hydrogels through hydrolytic and enzymatic degradation studies.
5) To evaluate the hemocompatibility and bioactivity of the developed hydrogels, including their ability to promote calcium-rich mineral deposition.
6) To explore the potential applicability of insulin-encapsulated hydrogels for advanced biomedical applications, such as wound healing, localized drug delivery, and tissue regeneration.

2.0. Materials and Methods

2.1. Materials

Commercial injectable insulin (NPH, 100 IU·mL^{-1}) was obtained from a local pharmacy in Saltillo, Mexico and used as received. Type I collagen was extracted from porcine dermis using a previously optimized protocol [14]. Hexamethylene diisocyanate (HDI), glycerol ethoxylate (GE, Mw ~1000 g·mol^{-1}), and L-tyrosine were used as precursors for the synthesis of the bioactive polyurethane crosslinker [15]. Ninhydrin, sodium hydroxide, and analytical-grade salts were purchased from commercial suppliers and used without further purification. Reagents required for degradation and biological assays, including pepsin and calcium salts, were also used as received.

2.2. Hydrogel Preparation

Collagen-based hydrogels were prepared under controlled conditions to ensure reproducibility. Briefly, collagen solutions (6 mg·mL^{-1}) were dispensed into 24-well plates and maintained at 4°C to prevent premature gelation [13]. Insulin was incorporated at different concentrations (15–60 µg per gel) (CL-I15, CL-I30 and CL-I60) under gentle mixing to ensure homogeneous distribution within the protein matrix. Subsequently, a bioactive waterborne polyurethane crosslinker was added at a fixed proportion relative to collagen (30 wt.%). The mixtures were mechanically homogenized at low temperature and then incubated at 37°C for 24 h to induce gelation and network formation [12,13]. The resulting hydrogels were obtained as stable three-dimensional matrices and used for further characterization.

2.3. Physicochemical Characterization

The structural and physicochemical properties of the hydrogels were evaluated using complementary techniques. Fourier-transform infrared spectroscopy (FTIR) was employed to identify functional groups and confirm chemical interactions within the network. Surface morphology was examined by scanning electron microscopy (SEM) using freeze-dried samples to evaluate pore architecture and microstructural features. The fatigue resistance of the hydrogels was evaluated under dynamic conditions by subjecting the samples to continuous agitation at controlled rotational speed for 72 h, corresponding to approximately 3.2×10^6 loading cycles. This approach was used to simulate prolonged cyclic mechanical stress. After testing, the structural integrity and deformation behavior of the hydrogels were assessed to determine their durability under repetitive loading conditions [16,17].

2.4. Gelation, Swelling, and Crosslinking Analysis

Gelation kinetics were monitored using a turbidity-based method by recording absorbance changes over time, providing insight into the rate and extent of network formation [16,17]. Swelling behavior was determined gravimetrically by comparing the hydrated and dry states of the hydrogels and expressed as percentage water uptake [12,13,16,17]. The swelling ratio was evaluated at different pH conditions (pH 4.5, 7.4, and 8.5) over a period of 3 days at 37°C to simulate physiologically relevant and pathological environments [8,10,14,17].

The degree of crosslinking was estimated indirectly using a ninhydrin assay, which quantifies residual free amine groups. A reduction in detectable amines relative to non-crosslinked collagen was interpreted as an increase in crosslinking density within the hydrogel network [12,13,16,17].

2.5. Degradation and Stability Studies

Hydrogel stability was evaluated under both hydrolytic and enzymatic conditions [12,13,16,17]. For hydrolytic degradation, samples were incubated in buffered solutions at different pH values (4.5, 7.4 and 8.5) to simulate physiological and pathological environments. Enzymatic degradation was assessed using proteolytic media containing pepsin (14 U per gel) at pH 4.5 and 7.4, representing acidic and physiological conditions, respectively. Mass loss was monitored over time to quantify degradation rates and evaluate the stability of the hydrogel network.

2.6. Hemocompatibility and Bioactivity Assessment

Hemocompatibility was evaluated by determining the hemolytic activity of the hydrogels following standard protocols based on ASTM F756-08. Briefly, hydrogel samples were incubated with human erythrocytes under controlled conditions at 37°C. After incubation, the samples were centrifuged, and the absorbance of the supernatant was measured spectrophotometrically to quantify hemoglobin release. The percentage of hemolysis was calculated relative to positive (complete hemolysis) and negative (no hemolysis) controls, allowing classification of the materials in terms of blood compatibility [13,15-18].

The potential bioactivity of the hydrogels was assessed through *in vitro* mineralization assays using simulated body fluid (SBF), prepared to mimic the ionic composition of human plasma. Pre-weighed hydrogel samples were immersed in SBF and incubated at 37°C under static conditions for a defined period (1 week). After incubation, mineral deposition or erosion was quantified gravimetrically by measuring mass changes.

Additionally, surface mineralization was qualitatively evaluated by Alizarin Red staining, which selectively binds calcium-rich deposits, providing visual evidence of mineral formation [18, 19]. The presence and nature of the deposited mineral phase were further analyzed using microscopy, confirming the formation of hydroxyapatite-like structures and indicating the potential bioactivity of the hydrogels [18,19].

2.7. Statistical Analysis

All experiments were conducted in triplicate, and results are presented as mean ± standard deviation. Statistical differences between groups were evaluated using one-way analysis of variance (ANOVA) followed by Tukey's post hoc test for multiple comparisons. A significance level of $p < 0.05$ was considered statistically significant.

3.0. Results and Discussion

3.1. Network Formation and Molecular Interactions

The gelation profiles, which reflect the progression of polymer network formation in the hydrogel state, are presented in Figure 2a. Overall, no major differences were observed in the initial nucleation stage among most formulations. CL, CL–I15, and CL–I60 exhibited rapid nucleation times of approximately 2 min, indicating fast onset of network formation. In contrast, CL–I30 showed a visible delay, with a nucleation time of around 12 min.

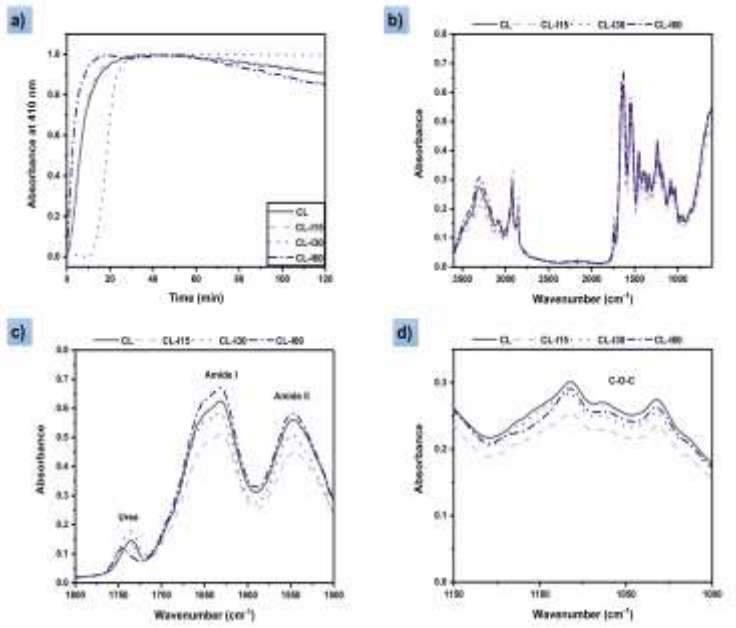

Figure 2. (a) Gelation profiles of hydrogels showing nucleation and network formation times. (b) FTIR spectra displaying characteristic functional groups and crosslinking interactions. (c) Enlarged view of urea and amide I–II regions highlighting differences in crosslinking degree and hydrogen bonding among formulations. (d) Enlargement of the C–O–C region indicating changes in polyurethane segment contribution in insulin-containing hydrogels.

This behavior suggests that higher insulin content can promote faster hydrogel formation, likely due to increased intermolecular interactions that facilitate early network assembly. The formation of a fully developed network was achieved at approximately 20 min for most systems, whereas CL–I30 required a longer time (≈29 min), consistent with its delayed nucleation. From an application perspective, these results are particularly relevant, as faster gelation can be advantageous in biomedical settings where rapid *in situ* formation is required, such as injectable systems or wound coverage, while still maintaining controlled network development [12,13,16-19].

The FTIR spectra of the hydrogels (Figure 2b) provide insight into the chemical interactions governing network formation. Characteristic bands associated with –OH and –NH stretching vibrations were observed between 3420 and 3100 cm^{-1}, while aliphatic –CH stretching appeared in the 2900–2700 cm^{-1} range. The presence of urethane/urea linkages, formed through the reaction between primary amine groups from the protein components and the electrophilic isocyanate groups of the polyurethane crosslinker, was identified around 1740 cm^{-1}. Additionally, the typical amide I, II, and III bands were detected at approximately 1680, 1580, and 1450 cm^{-1},

confirming the protein-based structure of the network [12-19]. Other contributions, including in-plane –NH and –CH vibrations (1400–1200 cm^{-1}) and C–O–C stretching from the ethoxylated glycerol segments (≈1100 cm^{-1}), further support the successful integration of all components into a hybrid system.

A closer inspection of the urea and amide regions (Figure 2c) reveals notable differences among formulations. The CL–I30 hydrogel exhibits a higher intensity of the urea-related band, suggesting a greater extent of crosslinking interactions at this composition. In contrast, CL–I60 shows a lower intensity, which may indicate that excess insulin partially hinders effective crosslink formation, likely due to steric effects or competition between intermolecular interactions. Variations in the intensity of amide I and II bands further suggest differences in hydrogen bonding, indicating that insulin content influences the organization and stability of the protein network [4,9,10,12,14-19].

In Figure 2d, the C–O–C region shows a decrease in intensity for all insulin-containing hydrogels compared to the control (CL). This behavior suggests that the presence of insulin alters the local environment of the polyurethane segments, potentially reducing their relative contribution to network organization. Interestingly, this observation aligns with the gelation results, where insulin-rich systems showed faster network formation, indicating that insulin not only participates in structural interactions but also modulates the kinetics of hydrogel assembly.

3.2. Morphology, Swelling Behavior, and Mechanical Stability

The macroscopic appearance of the hydrogels is shown in Figure 3a. As the insulin content increases, a noticeable expansion in the final hydrogel volume is observed. This behavior can be attributed to the hydrophilic nature of insulin, which enhances water uptake and promotes a more open network structure [20,21]. In general, all hydrogels gelled directly within the mold, adopting its shape. This feature is particularly advantageous for biomedical applications, as it enables in situ formation and precise adaptation to irregular geometries, such as wound sites or tissue defects [12,13,16-19].

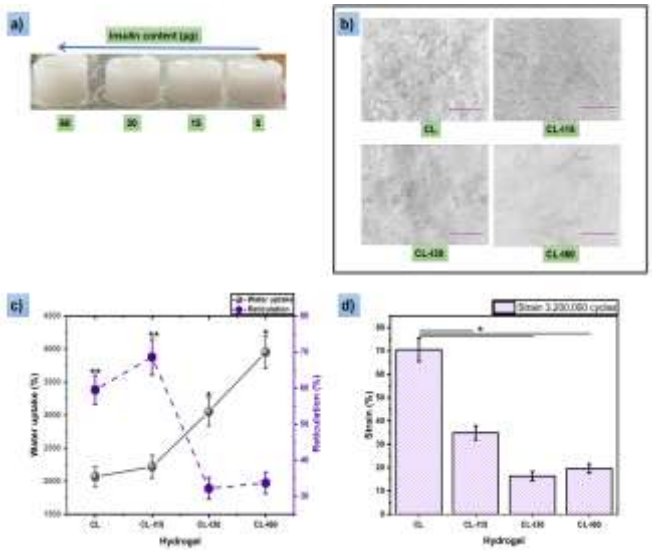

Figure 3. (a) Macroscopic appearance of hydrogels showing increased volume with insulin content and *in situ* mold adaptation. (b) SEM micrographs illustrating morphological changes from porous fibrillar structures to smoother and less porous surfaces with increasing insulin. (c) Swelling ratios/crosslinking degree, and (d) Mechanical deformation after cyclic fatigue (3,200,000 cycles), highlighting the effect of insulin on stability.

SEM micrographs (Figure 3b) reveal significant differences in surface morphology. The control hydrogel (CL) exhibits a porous, fibrillar, and highly interconnected structure, characteristic of a well-developed protein-based network [12,13,16-19]. With increasing insulin content, the surfaces become progressively smoother, accompanied by a reduction in apparent surface porosity. This effect may be explained by the ability of insulin to occupy free volume within the network and promote additional intermolecular interactions, leading to a more compact and less heterogeneous structure.

Notably, CL–I30 displays pronounced aggregation domains, suggesting enhanced protein–protein interactions coupled with polyurethane-mediated crosslinking. This observation is consistent with FTIR results, where a higher intensity of urea linkages indicates increased chemical interactions; however, these interactions appear to be more localized, generating heterogeneous domains rather than a uniformly crosslinked network.

The swelling and crosslinking behavior of the hydrogels is presented in Figure 3c. Swelling ratios of approximately 2100%, 2180%, 2800%, and 3800% were obtained for CL, CL–I15, CL–I30, and CL–I60, respectively, with statistically significant differences for higher insulin contents. The enhanced swelling capacity can be attributed to the increased hydrophilicity and osmotic driving force introduced by insulin, as well as to a less homogeneous network structure that facilitates water diffusion. This is also consistent with the delayed gelation observed for CL–I30, where a slower network formation may lead to structural rearrangements that favor water uptake.

Regarding crosslinking degree, values of 64% (CL), 72% (CL–I15), 36% (CL–I30), and 37% (CL–I60) were obtained, showing a significant decrease at higher insulin contents. This apparent contradiction with FTIR results, where CL–I30 exhibited stronger urea signals, can be explained by the nature of the assays. While FTIR detects the presence of specific chemical bonds, the ninhydrin-based method quantifies free amine consumption across the entire network. In the case of CL–I30, the higher local formation of urea linkages likely occurs within aggregated domains, as observed by SEM, rather than being uniformly distributed. As a result, the overall effective crosslinking density is lower, which also aligns with its delayed gelation behavior.

Mechanical stability under cyclic fatigue (3,200,000 cycles) is also shown in Figure 3d. Deformation values of 70% (CL), 35% (CL–I15), 14% (CL–I30), and 19% (CL–I60) were recorded, with significant differences between insulin-containing hydrogels and the control. The reduced deformation in insulin-loaded systems indicates improved resistance to mechanical stress, likely due to the formation of a hybrid network combining protein interactions and polyurethane crosslinking. This enhanced mechanical resilience is highly relevant for biomedical applications, where materials are subjected to repeated mechanical loads, such as in soft tissue environments [6,8, 14,16], wound dressings [13,17-19], or injectable scaffolds requiring structural integrity over time [11-13,16-19].

3.3. pH-Responsive Swelling Behavior and Environmental Stability

The equilibrium swelling profiles of the hydrogels under different hydrolytic conditions are presented in Figure 4. At acidic pH 4.5 (Figure 4a), which mimics skin-like conditions [16-19], all hydrogels reached their maximum swelling within the first day. Swelling values of approximately 3100% (CL), 3920% (CL–I15), 5100% (CL–I30), and 5530% (CL–I60) were observed, with significantly higher values for insulin-rich systems. This enhanced swelling can be attributed to the combined effect of increased hydrophilicity and a less homogeneous network

structure, as previously suggested by SEM and crosslinking results. In particular, the presence of insulin promotes water affinity and generates regions with lower effective crosslinking density, facilitating rapid fluid uptake. After the second day, equilibrium swelling was reached for all systems, with slightly reduced values (≈2800–4600%), indicating network relaxation and partial structural reorganization.

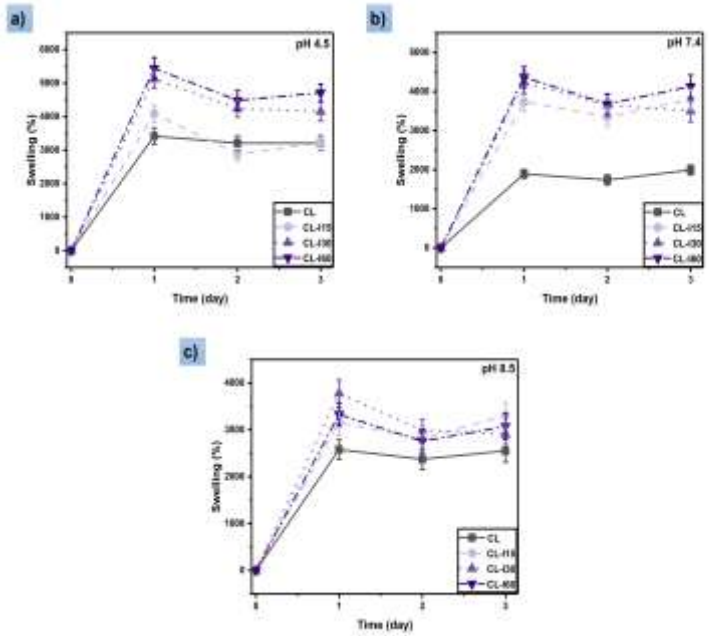

Figure 4. Swelling behavior of hydrogels under different pH conditions: (a) pH 4.5, (b) pH 7.4, and (c) pH 8.5, showing maximum and equilibrium swelling as a function of insulin content.

At physiological pH 7.4 (Figure 4b), a similar trend was observed, although with comparatively lower swelling capacities. Maximum swelling on day 1 reached approximately 1920% (CL), 3830% (CL–I15), 4200% (CL–I30), and 4480% (CL–I60), again showing significant differences between insulin-containing hydrogels and the control (CL). The reduced swelling compared to acidic conditions may be related to changes in the ionization state of functional groups within the network, leading to stronger intermolecular interactions and a more compact structure [13,16-19]. By day 2, equilibrium was achieved with values ranging from ~1900% to 3870%. This behavior suggests that while insulin enhances swelling across all conditions, the extent of water uptake remains sensitive to environmental pH.

Under alkaline conditions (pH 8.5, Figure 4c), the swelling behavior shows a distinct response. Maximum values at day 1 were approximately 2452% (CL), 3120% (CL–I15), 3860% (CL–I30), and 3342% (CL–I60), with CL–I30 exhibiting the highest swelling capacity. This result can be associated with its lower effective crosslinking degree and more heterogeneous structure, as previously observed in FTIR, SEM, and gelation analyses. In this case, the network appears to favor water diffusion despite localized crosslinking domains, resulting in enhanced swelling compared to more uniformly structured systems such as CL–I15. By day 2, equilibrium swelling values stabilized between ~2440% and 3100%, reflecting a balance between network expansion and structural constraints.

Overall, the hydrogels exhibit a clear pH-responsive swelling behavior, with higher water uptake under acidic conditions and composition-dependent responses under physiological and alkaline environments. These results are

consistent with the structural features observed previously, including surface morphology, crosslinking heterogeneity, and gelation kinetics. From an application standpoint, this behavior is highly relevant, as it suggests that insulin-loaded hydrogels can adapt their swelling capacity depending on the surrounding environment. In particular, the enhanced swelling at skin-like pH, combined with improved mechanical stability and controlled network structure, highlights their potential for applications such as wound dressings [13,16], localized drug delivery systems [12,13,17,19], and bioactive scaffolds [13,16-19].

3.4. Degradation Behavior and Environmental Stability

The degradation behavior of the hydrogels under hydrolytic and enzymatic conditions is presented in Figure 5. This evaluation is critical, as it determines the stability and lifetime of the materials in physiological environments, directly influencing their suitability for biomedical applications [5,9-13,16-19].

After 30 days under acidic conditions (pH 4.5, Figure 5a), degradation values of approximately 55% (CL), 43% (CL–I15), 48% (CL–I30), and 47% (CL–I60) were observed. The lower degradation of insulin-containing hydrogels compared to the control indicates that the formation of a hybrid network through polyurethane crosslinking enhances resistance to acidic hydrolysis. This improved stability can be attributed to the presence of urea linkages and stronger intermolecular interactions, which reinforce the network structure and maintain its integrity despite the high water uptake observed under acidic conditions.

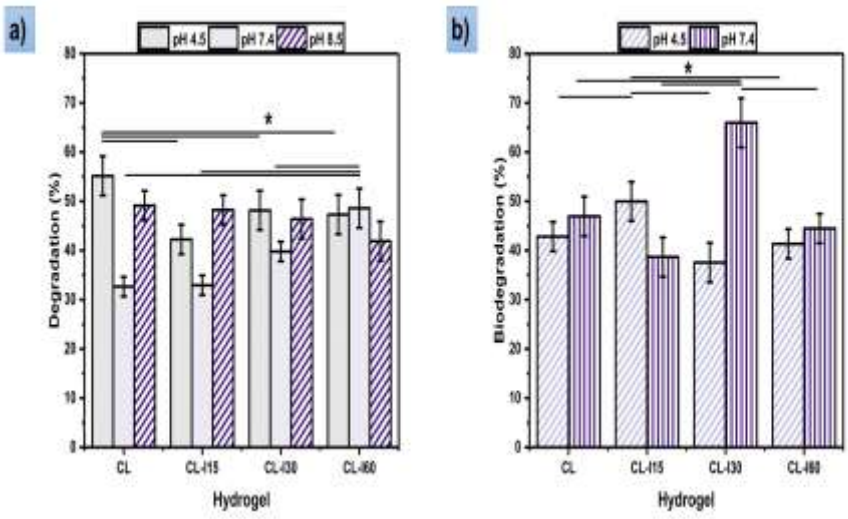

Figure 5. (a) Hydrolytic degradation of hydrogels at different pH conditions (4.5, 7.4, and 8.5) after 30 days. (b) Enzymatic degradation in the presence of pepsin at pH 4.5 and 7.4 after 30 days, showing the effect of insulin content on hydrogel stability.

At physiological pH 7.4, degradation values of 32% (CL), 33% (CL–I15), 47% (CL–I30), and 46% (CL–I60) were obtained, with significantly higher degradation for hydrogels with elevated insulin content. This behavior can be explained by the less homogeneous network structure and lower effective crosslinking degree observed at higher insulin concentrations. As discussed in previous sections, systems such as CL–I30 exhibit localized crosslinking domains and increased swelling capacity, which facilitate water diffusion and promote hydrolytic degradation under physiological conditions.

Under alkaline conditions (pH 8.5), degradation values ranged from 43% to 49% across all formulations, with no significant differences between systems. This suggests that the polyurethane-crosslinked hybrid network provides a stabilizing effect against alkaline hydrolysis, likely due to the relative chemical stability of urethane/urea linkages and the reduced sensitivity of the network structure to deprotonation effects at higher pH.

Enzymatic degradation in the presence of pepsin (Figure 5b) further highlights the role of insulin in modulating network behavior. At pH 4.5, biodegradation values of 43% (CL), 50% (CL–I15), 38% (CL–I30), and 41% (CL–I60) were observed. The higher degradation in CL–I15 suggests that lower insulin content leads to a more accessible and less protected network, allowing easier enzymatic attack. In contrast, higher insulin concentrations promote structural rearrangements, reduced porosity, and increased intermolecular interactions, as observed in SEM and FTIR analyses, which hinder enzyme diffusion and slow down biodegradation.

At physiological pH, enzymatic degradation showed a distinct behavior, with values of 47% (CL), 38% (CL–I15), 67% (CL–I30), and 44% (CL–I60). Notably, CL–I30 exhibited significantly higher biodegradation compared to the other systems. This can be attributed to its heterogeneous structure, characterized by localized crosslinking and higher swelling capacity, which facilitates enzyme penetration and accelerates matrix breakdown. This observation is consistent with previous findings on gelation delay, reduced effective crosslinking, and increased water uptake in this formulation.

These results demonstrate that insulin content plays a key role in tuning the degradation profile of the hydrogels by modulating network structure, crosslinking distribution, and swelling behavior. From an application perspective, this tunable degradation is highly advantageous, as it allows the design of materials with controlled stability depending on the target environment [13,16,17,19]. In particular, the balance between mechanical integrity, swelling capacity, and degradation rate makes these hydrogels promising candidates for applications such as wound healing [13,16], localized drug delivery [12,13,16,17,19], and bioactive scaffolds requiring gradual resorption [13, 16-19].

3.5. Hemocompatibility and Bioactivity

The hemocompatibility of the polyurethane-crosslinked double-protein hydrogels was evaluated through a hemolysis assay (Figure 6a), which quantifies hemoglobin release from erythrocytes as an indicator of membrane damage, following standard protocols [17-19]. The control hydrogel (CL) exhibited a hemolysis value of approximately 3%, whereas all insulin-containing systems showed negligible hemolytic activity (≈0%), with statistically significant differences between CL and the insulin-loaded hydrogels. This improved hemocompatibility can be attributed to the structural and surface modifications induced by insulin incorporation. As previously observed in SEM and swelling analyses, insulin promotes smoother and less porous surfaces, reducing direct mechanical interaction with erythrocyte membranes. Additionally, the formation of a more hydrated and stable interface likely minimizes protein adsorption and membrane disruption [18], contributing to the non-hemolytic behavior of the insulin-containing hydrogels.

The bioactivity of the hydrogels, defined as their ability to induce mineral formation under physiological-like conditions, was evaluated using SBF. After 7 days of incubation (Figure 6b), all systems exhibited surface erosion

associated with hydrolytic degradation processes, with mass losses of approximately 64% (CL), 59% (CL–I15), 60% (CL–I30), and 57% (CL–I60). The slightly lower erosion observed in insulin-containing hydrogels suggests that the hybrid network formed through polyurethane crosslinking and protein interactions provides enhanced resistance to degradation, consistent with the stability trends discussed previously.

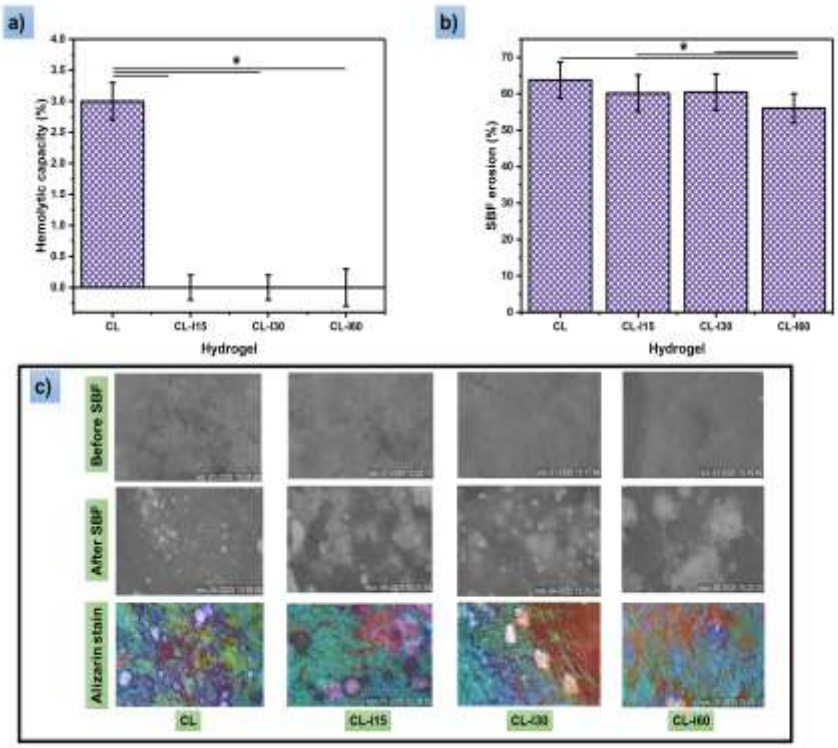

Figure 6. (a) Hemolytic activity of hydrogels showing improved hemocompatibility with insulin incorporation. (b) Surface erosion after 7 days in simulated body fluid (SBF). (c) Surface morphology before and after SBF exposure, and Alizarin Red staining indicating calcium-rich mineral deposition.

Microscopic analysis of the hydrogel surfaces before and after SBF exposure (Figure 6c) revealed significant changes. Prior to incubation, all hydrogels displayed the previously described morphologies, with increasing insulin content leading to more compact and granular surfaces due to enhanced fiber entanglement. After SBF exposure, opaque white deposits were observed on the hydrogel surfaces, indicating mineral formation. These deposits became more pronounced with increasing insulin content.

To further confirm the nature of these deposits, Alizarin Red staining was employed. This technique is based on the selective binding of the dye to calcium ions, producing an orange–reddish coloration in the presence of calcium-rich phases such as hydroxyapatite [18,19,22]. The insulin-containing hydrogels, particularly CL–I30 and CL–I60, exhibited more intense staining, suggesting a higher degree of calcium deposition and, therefore, enhanced bioactivity.

The increased mineralization observed in insulin-rich systems can be associated with their higher swelling capacity and more dynamic network structure, which facilitate ion diffusion and nucleation processes [18,19]. Although collagen inherently contains functional groups capable of nucleating calcium phosphate, the incorporation of insulin appears to enhance their effective availability and spatial distribution within the network. This, combined

with the increased swelling and structural heterogeneity observed in insulin-rich hydrogels, promotes ion diffusion and creates favorable microenvironments for mineral nucleation and growth. These findings are consistent with previous observations, where insulin was shown to modulate network architecture, promoting conditions favorable for mineral formation. From a biomedical view, the combination of hemocompatibility, controlled degradation, and the ability to induce hydroxyapatite-like deposition highlights the potential of these hydrogels as multifunctional biomaterials [18,19]. Their capacity to interact with biological fluids, support mineralization, and maintain structural integrity makes them promising candidates for applications such as wound healing [13,16-19], bioactive dressings [17-19], and scaffolds for tissue regeneration [12,13,16-19].

4.0. Conclusions

This study demonstrates that insulin encapsulation within collagen–polyurethane hydrogels not only enable its incorporation into a biomaterial matrix, but also actively modulates the structural, mechanical, and biological behavior of the system. Insulin content was found to play a key role in tuning gelation, network organization, swelling, and degradation properties. Higher insulin concentrations (30–60 µg) promoted increased swelling capacity (up to ~5530% under acidic conditions) and enhanced pH responsiveness, while lower insulin content (15 µg) favored a higher effective crosslinking degree (~72%), indicating a balance between network stability and structural heterogeneity. These differences were reflected in morphological and spectroscopic analyses, where insulin induced smoother, less porous surfaces and localized interactions within the hybrid network.

Importantly, insulin incorporation significantly improved mechanical performance, reducing deformation under cyclic fatigue (down to ~14–19% compared to ~70% for the control), while maintaining structural integrity under highly hydrated conditions. Degradation studies further revealed that insulin enhances stability in acidic environments, while enabling controlled degradation under physiological conditions through increased network accessibility. All insulin-containing hydrogels exhibited excellent hemocompatibility (~0% hemolysis), along with the ability to promote calcium-rich mineral deposition, particularly at higher insulin contents. This enhanced bioactivity is associated with increased swelling, structural reorganization, and improved ion diffusion within the matrix. Overall, insulin acts as a multifunctional component that extends beyond its therapeutic role, enabling the design of responsive, mechanically stable, and bioactive hydrogel systems. These findings highlight the potential of collagen–polyurethane–insulin hydrogels as promising candidates for advanced biomedical applications, including wound healing, localized drug delivery, and tissue regeneration.

4.1. Future Suggestions

Despite the promising results, some limitations should be considered for the successful translation of these hydrogels into biomedical applications.

(i) Conduct in vivo studies to validate the performance and biocompatibility of the insulin-loaded collagen hydrogels under complex physiological conditions.

(ii) Perform a more comprehensive biological evaluation, including long-term cytocompatibility, cell proliferation, and cellular response assays.

(iii) Investigate the release profile of encapsulated insulin and assess the preservation of its biological activity after incorporation into the hydrogel matrix.

(iv) Evaluate the scalability and reproducibility of the hydrogel fabrication process to ensure consistency for potential large-scale production.

(v) Assess the long-term mechanical stability and degradation behavior of the hydrogels under dynamic physiological environments.

(vi) Explore the applicability of these hydrogels in specific biomedical fields, such as tissue engineering, regenerative medicine, and advanced wound care.

Declarations

Source of Funding

This study did not receive any grant from funding agencies in the public or not-for-profit sectors.

Competing Interests Statement

The authors declare that they have no conflict of interest.

Consent for Publication

The authors declare that they consented to the publication of this study.

Authors' contributions

All the authors took part in literature review, analysis, and manuscript writing equally.

Informed Consent

Not applicable.

Availability of Data and Material

The data supporting the findings of this study are available from the corresponding author upon reasonable request.

Institutional Review Board Statement

Not applicable.

Ethical Approval

Not applicable.

Acknowledgements

The authors thank the Secretariat of Science, Humanities, Technology and Innovation (SECIHTI) for the postgraduate scholarships awarded to the students involved in this study.

Declaration of Artificial Intelligence

The authors used ChatGPT (OpenAI) as a language assistance tool exclusively for grammar correction, language refinement, and improvement of manuscript structure. The AI tool was not used for data analysis, interpretation of results, generation of scientific conclusions, or preparation of figures and experimental content. The authors reviewed, verified, and take full responsibility for the final content of the manuscript.

References

[1] Lee, S.H., & Yoon, K.H. (2021). A century of progress in diabetes care with insulin: A history of innovations and foundation for the future. Diabetes & Metabolism Journal, 45(5): 629–640. https://doi.org/10.4093/dmj.2021.0163.

[2] Li, M., Chi, X., Wang, Y., Setrerrahmane, S., Xie, W., & Xu, H. (2022). Trends in insulin resistance: Insights into mechanisms and therapeutic strategy. Signal Transduction and Targeted Therapy, 7(1): 216. https://doi.org/10.1038/s41392-022-01073-0.

[3] Riachi, R., Khalife, E., Kędzia, A., & Niechciał, E. (2025). Understanding insulin actions beyond glycemic control: A narrative review. Journal of Clinical Medicine, 14(14): 5039. https://doi.org/10.3390/jcm14145039.

[4] Sun, Q., Li, J., & Gao, F. (2014). New insights into insulin: The anti-inflammatory effect and its clinical relevance. World Journal of Diabetes, 5(2): 89–96. https://doi.org/10.4239/wjd.v5.i2.89.

[5] Cerasuolo, M., Auriemma, M.C., Di Meo, I., Lenti, C., Papa, M., Paolisso, G., & Rizzo, M.R. (2025). Understanding the insulin-degrading enzyme: A new look at Alzheimer's disease and Aβ plaque management. International Journal of Molecular Sciences, 26(14): 6693. https://doi.org/10.3390/ijms26146693.

[6] Hornsby, B.D., Lee, C.H., Steele, C.A., Tuekpe, J.K.K., & Lim, C.S. (2026). Therapeutic peptides and proteins: Status and developments in drug delivery. Journal of Controlled Release, 394: 114895. https://doi.org/10.1016/j.jconrel.2026.114895.

[7] Baral, K.C., & Choi, K.Y. (2025). Barriers and strategies for oral peptide and protein therapeutics delivery: Update on clinical advances. Pharmaceutics, 17(4): 397. https://doi.org/10.3390/pharmaceutics17040397.

[8] Ghazwani, M., Hani, U., Kyada, A., Ballal, S., Issa, B.S., Abosaoda, M.K., Singh, A., Sabarivani, A., & Ray, S. (2025). Advancements in insulin delivery: The potential of natural polymers for improved diabetes management. Frontiers in Bioengineering and Biotechnology, 13: 1566743. https://doi.org/10.3389/fbioe.2025.1566743.

[9] Mansoor, S., & Kondiah, P.P.D. (2021). Advanced hydrogels for the controlled delivery of insulin. Pharmaceutics, 13(12): 2113. https://doi.org/10.3390/pharmaceutics13122113.

[10] Li, L., & Wang, Y. (2025). Advancements in injectable hydrogels for controlled insulin delivery: A comprehensive review of the design, properties and therapeutic applications for diabetes and its complications. Polymers, 17(6): 780. https://doi.org/10.3390/polym17060780.

[11] Chaturvedi, K., Ganguly, K., Nadagouda, M.N., & Aminabhavi, T.M. (2013). Polymeric hydrogels for oral insulin delivery. Journal of Controlled Release, 165(2): 129–138. https://doi.org/10.1016/j.jconrel.2012.11.005.

[12] Rangel-Argote, M., Claudio-Rizo, J.A., Castellano, L.E., Vega-González, A., Mata-Mata, J.L., & Mendoza-Novelo, B. (2017). ECM–oligourethene–silica hydrogels as a local drug release system of dexamethasone for stimulating macrophages. RSC Advances, 7(17): 10443–10453. https://doi.org/10.1039/c6ra25989h.

[13] León-Campos, M.I., Claudio-Rizo, J.A., Cobos-Puc, L.E., Cabrera-Munguía, D.A., Rubio-Rios, A., Oyervides-Muñoz, E., & Velázquez-Arrellano, A. (2025). Nanostructured polyurethane-collagen hydrogels: Bioactive crosslinked networks for enhanced wound healing. Journal of Biomedical Materials Research Part A, 113(10): e37993. https://doi.org/10.1002/jbm.a.37993.

[14] Claudio-Rizo, J.A., Rangel-Argote, M., Castellano, L.E., Delgado, J., Mata-Mata, J.L., & Mendoza-Novelo, B. (2017). Influence of residual composition on the structure and properties of extracellular matrix-derived hydrogels. Materials Science and Engineering C, 79: 793–801. https://doi.org/10.1016/j.msec.2017.05.118.

[15] León-Campos, M.I., Claudio-Rizo, J.A., Cabrera-Munguía, D.A., Cobos-Puc, L.E., Caldera-Villalobos, M., González-Díaz, M.O., & Enríquez-Medrano, F.J. (2024). Development of novel bioactive waterborne polyurethanes: Effect of polyurethane chemical structure on its properties. Journal of Polymer Research, 31(7): 213. https://doi.org/10.1007/s10965-024-04055-8.

[16] León-Campos, M.I., Claudio-Rizo, J.A., Becerra-Rodriguez, J.J., González-Díaz, M.O., Flores-Guía, T.E., Soriano-Corral, F., & Herrera-Guerrero, A. (2025). Novel tragacanth gum-collagen-polyurethane hydrogels: Super-swelling, antibacterial, and fibrillogenesis-enhancing properties for efficient wound healing. International Journal of Biological Macromolecules, 310(Pt. 1): 143281. https://doi.org/10.1016/j.ijbiomac.2025.143281.

[17] Usme-Duque, L.K., Medina-Morales, M.A., León-Campos, M.I., et al. (2026). Fermented plant extract-loaded collagen scaffolds: Bioactive hydrogels for enhanced wound repair and immune modulation. Gels, 12(2): 129. https://doi.org/10.3390/gels120 20129.

[18] Oyervides-Guajardo, V.G., Claudio-Rizo, J.A., León-Campos, M.I., Cabrera-Munguía, D.A., González-Díaz, M.O., Soriano-Corral, F., Herrera-Guerrero, A., & Sierra-Rivera, C.A. (2026). Biomimetic double-protein semi-IPN hydrogels: Synergistic protein-polysaccharide biomatrices for healing, immunomodulation, and mineralization. Biopolymers, 117(3): e70089. https://doi.org/10.1002/bip.70089.

[19] Mendoza-Villafaña, J.J., Claudio-Rizo, J.A., León-Campos, M.I., Becerra-Rodríguez, J.J., Rodríguez-Fuentes, N., Betancourt-Galindo, R., Cabrera-Álvarez, E.N., & Cano-Salazar, L.F. (2026). Collagen-polyurethane-maltodextrin hydrogels as bioactive scaffolds for soft and hard tissue regeneration, immunomodulation, and drug delivery. International Journal of Biological Macromolecules, 338(Pt. 2): 149718. https://doi.org/10.1016/j.ijbiomac.2025.149718.

[20] Gerlough, T.D., & Bates, R.W. (1932). The purification and some properties of insulin. The Journal of Pharmacology and Experimental Therapeutics, 45(1): 19–51.

[21] Norrman, M., Hubálek, F., & Schluckebier, G. (2007). Structural characterization of insulin NPH formulations. European Journal of Pharmaceutical Sciences, 30(5): 414–423. https://doi.org/10.1016/j.ejps.2007.01.003.

[22] Bernar, A., Gebetsberger, J.V., Bauer, M., Streif, W., & Schirmer, M. (2022). Optimization of the Alizarin Red S assay by enhancing mineralization of osteoblasts. International Journal of Molecular Sciences, 24(1): 723. https://doi.org/10.3390/ijms24010723.